

Supplementary Materials for:

The effects of β -lactam antibiotics on surface modifications of multidrug-resistant *Escherichia coli*:

A multiscale approach

Samuel C. Uzoечи¹ and Nehal I. Abu-Lail^{2}*

¹Gene and Linda Voiland School of Chemical Engineering and Bioengineering, Washington

State University, Pullman, WA 99164

²Department of Biomedical Engineering, The University of Texas at San Antonio, San Antonio, TX, 78249

***Corresponding Author:**

Nehal I. Abu-Lail
Department of Biomedical Engineering
The University of Texas at San Antonio
One UTSA Circle
AET 1.102
San Antonio, TX, 78249
210-458-8131
nehal.abu-lail@utsa.edu

Summary of Content

Number of Pages: 14

Number of Figures: 6

Number of Tables: 2

S.1 Morphology of Cells as a Function of Ampicillin Treatment as Imaged by AFM. MDR-E.

coli cells, representative of the different strains investigated, were imaged under DI water with a Multimode AFM equipped with a Nanoscope IIIa controller and extender module (Bruker AXS Inc.) before and after being exposed to various MICs of ampicillin ~~with a Multimode AFM equipped with a Nanoscope IIIa controller and extender module (Bruker AXS Inc.)~~. The AFM height [Error! Reference source not found.Figure S1A inset] and phase images were captured concurrently in every single scan. Using the standard AFM Nanoscope Analysis 1.5 software (Bruker, Camarillo, CA), the dimensions (length, width, and height) of individual bacterial cells were characterized for each treatment. To obtain the dimensions, sectional lines were traced on the bacterial images as shown in Error! Reference source not found.Figure S1A. The surface area (SA) and surface area to volume ratio (SA/V) of individual cells were estimated by approximating cells as ellipsoids. The surface area and volume of an ellipsoid are given by:

$$SA = 4\pi \left(\frac{(ab)^{1.6} + (ac)^{1.6} + (bc)^{1.6}}{3} \right)^{1/1.6} \quad (S1)$$

$$V = \frac{4}{3} \pi abc \quad (S2)$$

The letters **a**, **b** and **c** describe the semi-axes from the origin of the ellipsoid to its surface and represents here length, width, and height, respectively as shown in Error! Reference source not found.Figure S1B.

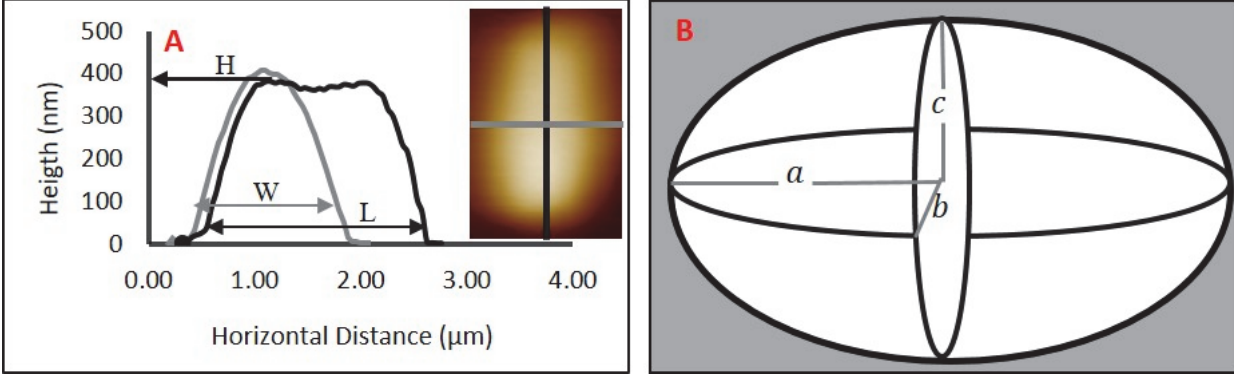


Figure S1: The gray and black section lines to the left correspond the same colors shown on the image in the inset. The cross sections can be analyzed to get the length (L), width (W) and maximum height (H) of the bacterial cell. (B) A three-dimensional schematic of an ellipsoid that models the dimensions of bacteria introduced in equations S1 and S2.

S.2 Analysis of the Surface Roughness of Individual Bacterial Cells. The surface roughness values of individual MDR-*E. coli* cells were estimated using data obtained from the AFM height images of individual cells. Using the freely-available online Gwyddion v2.17 software (gwyddion.net), the root-mean-square roughness (RMS) was determined over a constant $0.60 \times 0.60 \mu\text{m}^2$ area for each bacterium surface (Alves *et al.*, 2010; Girasole *et al.*, 2007). The RMS of the height distribution is represented by Equation S3.

$$R_{\text{RMS}} = \sqrt{\sum_{i=1}^N \frac{(Z_i - Z_{\text{ave}})^2}{N - 1}} \quad (\text{S3})$$

Where N is the number of data points measured within a given area, Z_i is the current height value, and Z_{ave} is the average height value within a given area (Alves *et al.*, 2010; Girasole *et al.*, 2007).

S.3 Contact Angle Measurements of Bacterial Cells. Cells harvested at the late exponential phase of growth were centrifuged and washed three times in 0.2 μm filtered DI water. Bacterial pellets were resuspended in DI water and filtered through a cellulose filter membrane with a pore diameter of 0.45 μm (Sartorius, Aubagne, France) using negative pressure (Park and Abu-Lail, 2011). The bacterial lawns formed on the filter membrane were placed in a Petri-dish containing 1% (w/v) Bacto agar (Difco, Detroit, Michigan) prepared in filtered DI water supplemented with 10% glycerol to maintain a constant moisture during the measurements. Bacterial contact angles of the suspended lawns were measured using three probe liquids with different polarities. These were ultrapure water, H_2O (polar, 18.2 $\text{m}\Omega\text{ cm}$ and $\epsilon = 78.5\%$), Formamide, CH_3NO (polar, $\epsilon = 111$, 99.5%) and Diiodomethane, CH_2I_2 (apolar, $\epsilon = 5.32$, 99%). ϵ refers to the dielectric constant of the solvent. A 1 μL droplet volume of each of the three probe liquids was dropped on the bacterial lawn with at least 10 – 20 different locations tested. Contact angles of the liquid drops formed on the bacterial lawns were then determined using a contact angle analyzer (AST product Inc., Billerica, MA). The volume of the probe liquid drop is much larger than the roughness of the lawn and as such roughness did not affect our contact angles measured (Park and Abu-Lail, 2011). The contact angles were measured within 15-20 minutes before the drying time of each bacterial strain. Drying time for *MDR-E. coli* lawns were determined to be ~ 25 minutes. The drying time is described as the time needed for the water contact angles to reach a plateau with time and depicts that the moisture of the cellular exterior is evaporated while the cells are not dehydrated (Park and Abu-Lail, 2011).

S.4 Surface Free Energy Calculations. Interfacial polar Lewis acid-base (AB) and apolar Lifshitz-van der Waals (LW) surface interactions have been proposed to govern the initial steps of bacterial adhesion (Israelachvili, 2011). The LW and AB surface interactions consist of electron-

acceptor (γ_s^+) and electron-donor (γ_s^-) interaction components (Van Oss, 2003). The polar and apolar components of the surface free energy are additive and are described by equations S4 and S5, (Van Oss, 2003).

$$\gamma_s = \gamma_s^{LW} + \gamma_s^{AB} \quad (S4)$$

$$\gamma_s^{AB} = 2\sqrt{\gamma_s^+ \gamma_s^-} \quad (S5)$$

Where, γ_s^{LW} and γ_s^{AB} (apolar or Lifshitz-van der Waals and polar or Lewis acid-base), γ_s is the total free energy of component and γ_s^- and γ_s^+ are the electron donor and acceptor of surface free energy components, respectively. The latter two can be obtained by solving the Young-Dupré equation of contact angle (θ) (Equation S6) (Van Oss, 2003). The subscripts S and L refer to bacterial and liquid phases.

$$\gamma_L(1+\cos \theta) = 2\left(\sqrt{\gamma_s^{LW} \gamma_L^{LW}} + \sqrt{\gamma_s^+ \gamma_L^-} + \sqrt{\gamma_s^- \gamma_L^+}\right) \quad (S6)$$

S.5 AFM Force Measurements

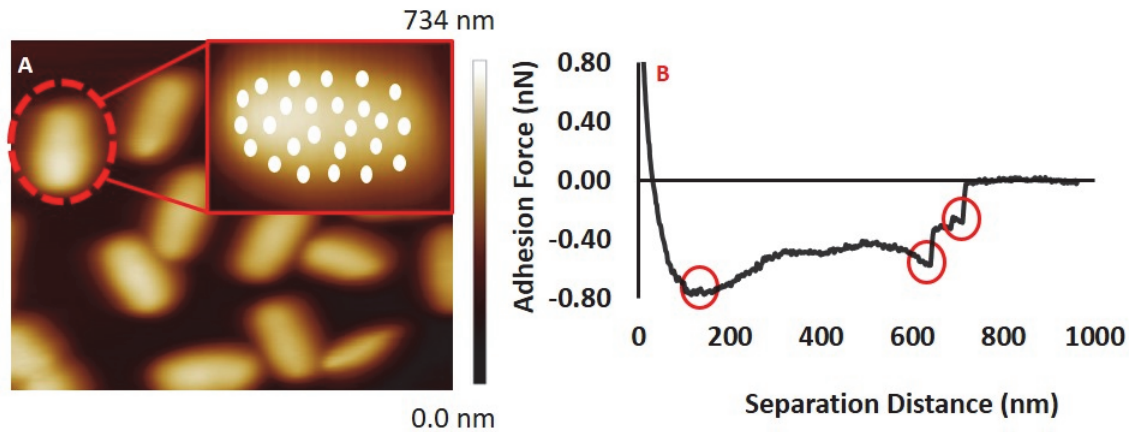


Figure S12: A representative tapping mode image of *E. coli* A5 cells attached to gelatin-coated mica under water. The inset shows how the 25 points were distributed onto the surface of a representative cell. The large image is $10 \times 10 \mu\text{m}^2$. (B) A representative example of a retraction curve obtained between the Si_3N_4 cantilever and the surface biopolymers of MDR-*E. coli* A5 strain with red circles indicating locations of adhesion forces.

S.6 Quantification of bacterial Biofilm Strength

Table S1: The categories of MDR *E. coli* biofilms as estimated following the approach established by [Stepanovic et al., 2007](#). OD_c is the average absorbance of the negative control and OD is the final optical density value of a tested strain. When OD is higher than OD_c , a biofilm has formed in the well.

Categories of Biofilm Formation	Criterion adopted
Strong biofilm former (+++)	$4 \times \text{OD}_c < \text{OD}$
Moderate biofilm former (++)	$2 \times \text{OD}_c < \text{OD} \leq 4 \times \text{OD}_c$
Weak biofilm former (+)	$\text{OD}_c < \text{OD} \leq 2 \times \text{OD}_c$
None biofilm former (0)	$\text{OD} \leq \text{OD}_c$

S.7 Effect of Ampicillin on Bacterial Morphology

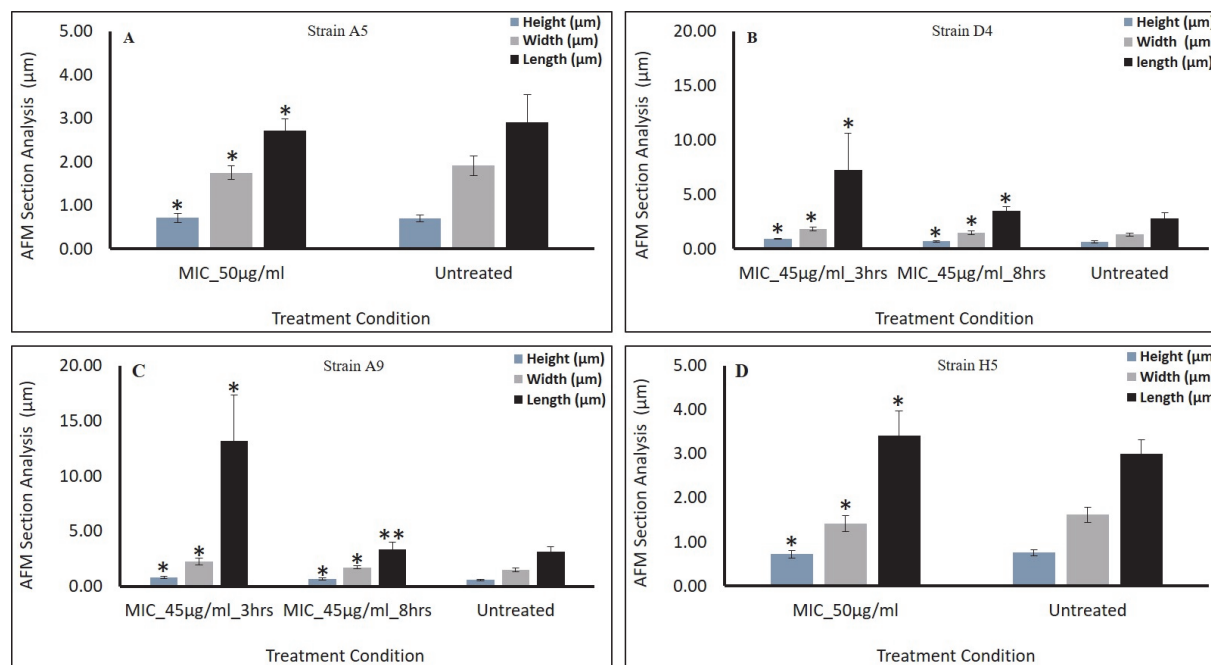


Figure S3: Summary of the dimensions of bacterial cells as analyzed with the AFM Nanoscope Analysis 1.5 software (Bruker, Camarillo, CA). Strains A5 and H5 were treated in the presence of ampicillin at 50 µg/ml MIC and strains D4 and A9 were treated at 45 µg/ml MIC. (A) Data for strain A5 with a total of 36 cells treated for 3 hours and untreated 44 cells. (B) Data for strain D4 with a total of 24 cells treated for 3 hours, 27 cells treated for 8 hours and 31 untreated cells. (C) Data for strain A9 with a total of 21 cells treated for 3 hours, 13 cells treated for 8 hours, and 25 untreated cells. (D) Data for strain H5 with a total of 31 treated cells for 3 hours and 44 untreated cells. *Values are statistically significant between the untreated and treated cells. ** Values statistically significant from the treated cells but not from the untreated cells, $p < 0.001$, $n = 3$ independent cultures.

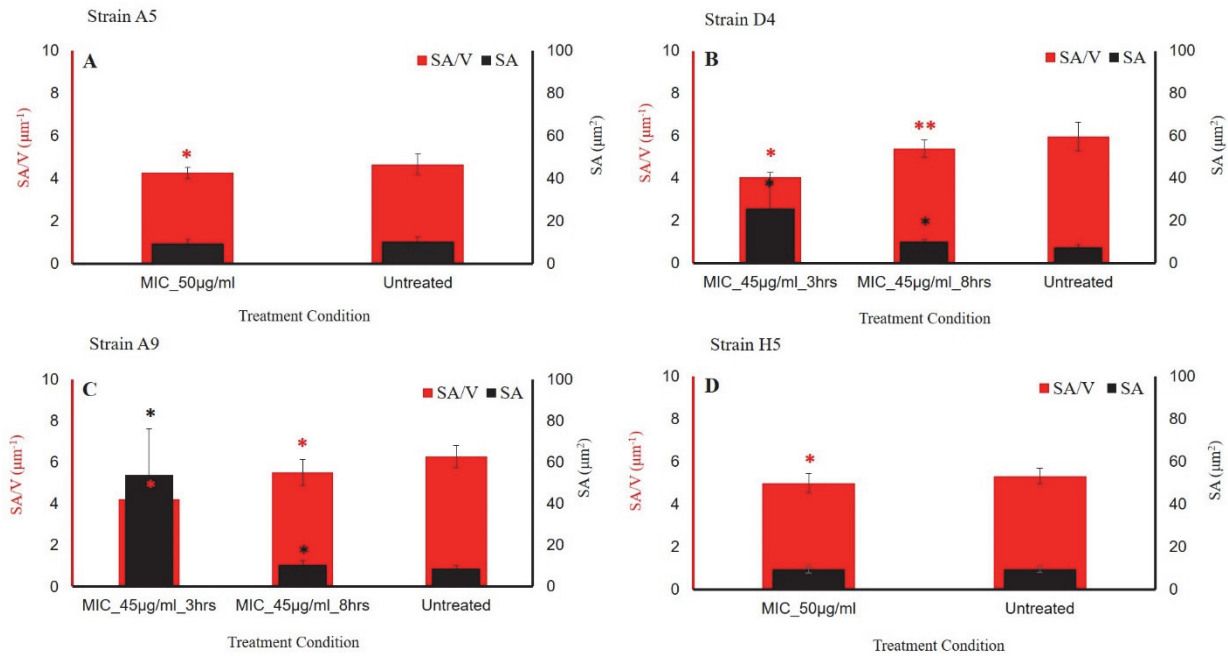


Figure S4: Summary of the average surface area (black) and surface area to volume ratio (gray) of each MDR-*E. coli* strain before and after exposure to ampicillin at strains' corresponding MICs. (A) Data for strain A5 with a total of 36 cells treated for 3 hours and untreated 44 cells. (B) Data for strain D4 with a total of 24 cells treated for 3 hours, 27 cells treated for 8 hours and 31 untreated cells. (C) Data for strain A9 with a total of 21 cells treated for 3 hours, 13 cells treated for 8 hours, and 25 untreated cells. (D) Data for strain H5 with a total of 31 treated cells for 3 hours and 44 untreated cells. *Values are statistically significant between the untreated and treated cells. ** Values statistically significant from the treated cells but not from the untreated cells, $p < 0.001$, $n = 3$ independent cultures.

S.8 Fluorescence Imaging of Cells as a Function of Ampicillin Treatment. Figure S5 shows fluorescence microscopy images of individual bacterial cells before and after exposure to ampicillin at the appropriate MIC (50 or 45 $\mu\text{g/ml}$). Upon exposure to 50 $\mu\text{g/ml}$ ampicillin for 3 hours, images of strain A5 indicated a reduction in the length of cells compared to cellular length

with no ampicillin exposure [Figures S5A and S5E]. Strains D4 and A9 images clearly show the elongation of the bacterial cells as they got exposed to ampicillin at MIC for 3 hours compared to their untreated with no ampicillin exposure [Figures S5B to S5F and S5C to S5G]. With ampicillin at 45 or 50 $\mu\text{g}/\text{ml}$ treatments for 3 hours, elongation was observed in strains D4, A9 and H5 compared to their untreated cells [Figures S5B, S5C, and S5D]. The results of fluorescence imaging are consistent with dimensions and observations obtained from AFM height images [Error! Reference source not found.Figure 2].

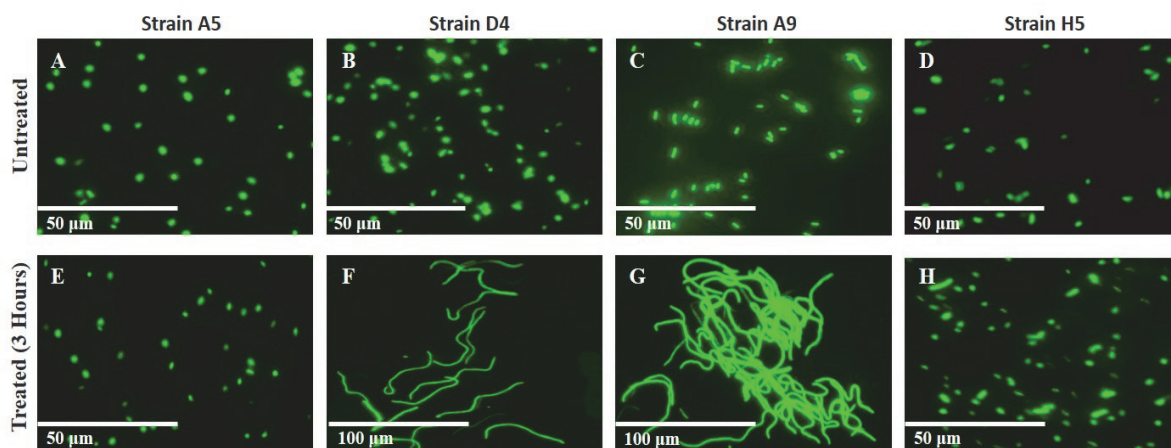


Figure S5: Representative images of the four MDR-*E. coli* strains incubated without (A-D) and with ampicillin for 3 hours at 50 $\mu\text{g}/\text{ml}$ (E and H) and at the 45 $\mu\text{g}/\text{ml}$ (F and G) above CLSI resistance breakpoint concentration.

According to Error! Reference source not found.Figure S5 images, no cell lysis was observed, and the elongated cells never released their DNA content. It has been reported that antibiotic concentrations that result in cell lysis induced release of DNA which rapidly binds to the SYTO 9 nucleic acid dye and appears clearly in the background of the fluorescent images (Bou *et al.*, 2012). The images presented in Error! Reference source not found.Figure S5 did not show any spread of DNA in the background. We realize that washing with PBS may cover the effects of possible cell lysis as DNA from lysed cells can get solubilized in water and washed away.

However, running these assays without washing adversely affects the resolution of the images. We felt it is necessary to remove the cell debris and non-adherent cells by washing for a better resolution (Yoon et al., 2011).

S.9 Effect of Ampicillin on Bacterial Surface Roughness, Membrane Permeability, Biofilm Formation and Adhesion Forces of MDR-*E. coli*.

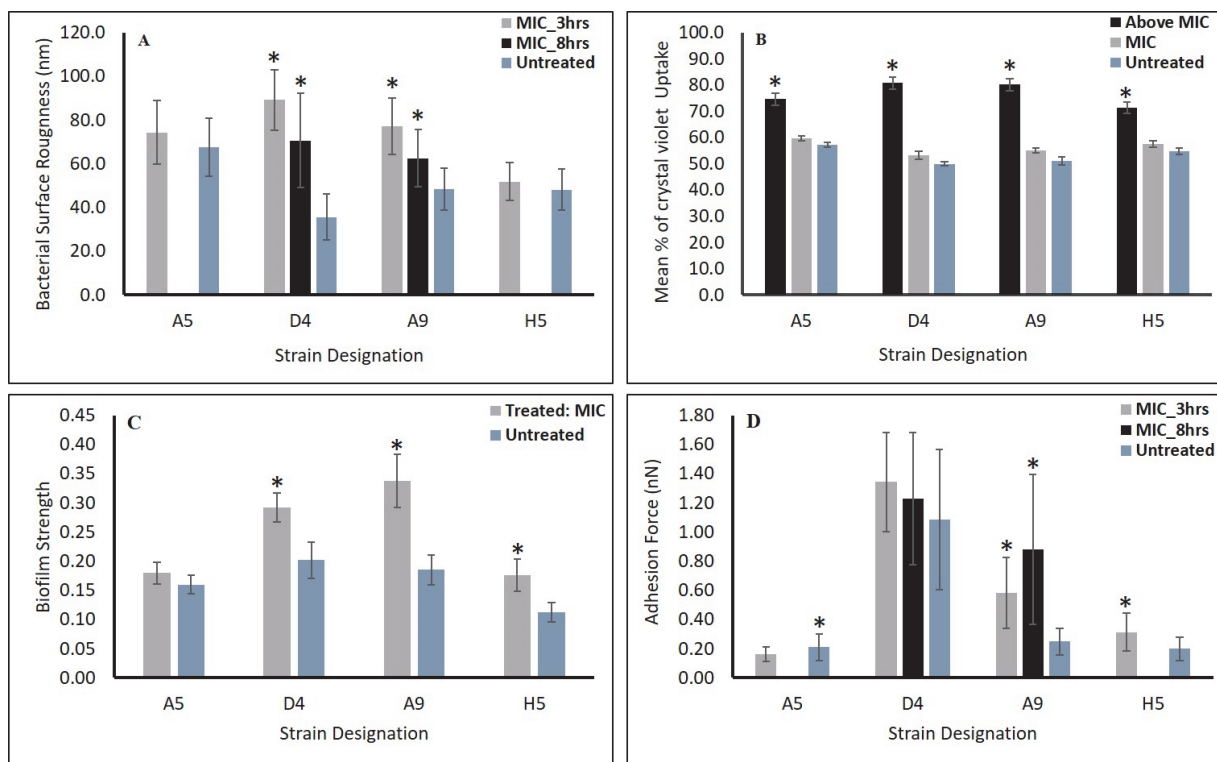


Figure S6: Summary of the effects of ampicillin exposure at relevant MICs on the surface characteristics of the MDR-*E. coli* strains investigated at variable exposure time points. (A) The average bacterial surface RMS (nm). (B) Summary of cellular membrane permeability (MP, %). (C) The average macroscale bacterial biofilm formation of cells. (D) Summary of the average AFM nanoscale adhesion force (F_{ad}) measured between the Si_3N_4 cantilever and the bacterial surface biopolymers. *Values are statistically significant from the control and treatment group at $p < 0.001$,

n = 3 independent cultures. MIC is (50 or 45 $\mu\text{g/ml}$) for strains A5 and H5, and D4 and A9 respectively. Above MIC is (65 or 55 $\mu\text{g/ml}$) for strains A5 and H5, and D4 and A9 respectively.

S.10 Effect of Ampicillin on Bacterial Surface Hydrophobicity.

Table S2: Contact angles of the bacterial strains measured in water, formamide and diiodomethane and the corresponding surface energy components (mJ/m^2). Contact angles were measured for cells untreated with ampicillin as well as for cells treated with ampicillin at the corresponding MIC for 3 hours. The reported contact angles are the means \pm standard deviations measured on 15 locations on a given bacterial lawn, * Values are statistically significant from the control, $p < 0.001$. NT = not treated, $n=3$ independent cultures.

Strain ID		^a Contact angle ($^\circ$)			^b Surface energy component (mJ/m^2)				
		θ^W	θ^D	θ^F	γ_s^{LW}	γ_s^+	γ_s^-	γ_s^{AB}	γ_s
A5	50	26 \pm 1	78 \pm 5*	25 \pm 1*	18.7	8.5	45.7	39.4	58.1
	NT	28 \pm 3	58 \pm 3	28 \pm 1	29.6	2.8	41.1	29.1	54.4
D4	45	29 \pm 2*	89 \pm 9*	33 \pm 4*	13.1	10.6	47.4	44.7	57.9
	NT	32 \pm 2	66 \pm 8	25 \pm 2	25.4	5.1	41.1	29.1	54.4
A9	45	21 \pm 1	74 \pm 9	24 \pm 1*	20.8	6.9	50.2	37.2	58.0
	NT	22 \pm 2	66 \pm 7	21 \pm 3	25.3	5.2	48.7	31.8	57.1
H5	50	28 \pm 2*	62 \pm 5	25 \pm 3	27.3	4.1	45.2	27.1	54.4
	NT	26 \pm 2	59 \pm 2	25 \pm 2	29.0	3.3	47.3	25.1	54.1

¹ θ^W , θ^D , and θ^F are the contact angles of water, diiodomethane, and formamide on MDR-*E. coli* respectively.

² γ_s^{LW} and γ_s^{AB} (Lifshitz-van der Waals and Lewis acid-base) and γ_s^+ and γ_s^- are the electron acceptor and donor of surface free energy components of MDR-*E. coli* respectively.

References

Alves, C. S. *et al.* (2010) 'Escherichia coli cell surface perturbation and disruption induced by antimicrobial peptides BP100 and pepR', *Journal of Biological Chemistry*, 285(36), pp. 27536–27544. doi: 10.1074/jbc.M110.130955.

Bou, G. *et al.* (2012) 'Fast assessment of resistance to carbapenems and ciprofloxacin of clinical strains of Acinetobacter baumannii', *Journal of Clinical Microbiology*, 50(11), pp. 3609–3613. doi: 10.1128/JCM.01675-12.

Girasole, M. *et al.* (2007) 'Roughness of the plasma membrane as an independent morphological parameter to study RBCs: A quantitative atomic force microscopy investigation', *Biochimica et Biophysica Acta - Biomembranes*, 1768(5), pp. 1268–1276. doi: 10.1016/j.bbamem.2007.01.014.

Israelachvili, J. (2011) *Intermolecular and Surface Forces, Intermolecular and Surface Forces*. doi: 10.1016/C2009-0-21560-1.

Van Oss, C. J. (2003) 'Long-range and short-range mechanisms of hydrophobic attraction and hydrophilic repulsion in specific and aspecific interactions', *Journal of Molecular Recognition*, 16(4), pp. 177–190. doi: 10.1002/jmr.618.

Park, B. J., and Abu-Lail, N. I. (2011) 'The role of the pH conditions of growth on the bioadhesion of individual and lawns of pathogenic *Listeria monocytogenes* cells', *Journal of Colloid and Interface Science*. Elsevier Inc., 358(2), pp. 611–620. doi: 10.1016/j.jcis.2011.03.025.

Stepanovic, S. *et al.* (2007) 'Quantification of Biofilm in Microtiter Plates: Overview of Testing Conditions and Practical Recommendations for Assessment of Biofilm Production by *Staphylococci*', *Apmis*, 115(3), pp. 891–899.

Yoon, M. Y. *et al.* (2011) 'Contribution of cell elongation to the biofilm formation of

Pseudomonas aeruginosa during anaerobic respiration', *PLoS ONE*, 6(1), pp. 1–11. doi:
10.1371/journal.pone.0016105.